Quantitative elastography provided by surface acoustic waves measured by phase-sensitive optical coherence tomography

Chunhui Li,[1,2] Guangying Guan,[1,2] Xi Cheng,[1] Zhihong Huang,[2] and Ruikang K. Wang[1,*]

[1]*Department of Bioengineering, University of Washington, 3720 15th Avenue Northeast, Seattle, Washington 98195, USA*

[2]*Division of Mechanical Engineering and Mechatronics, University of Dundee, Dundee DD1 4HN, Scotland, UK*

**Corresponding author: wangrk@u.washington.edu*

Received December 9, 2011; accepted January 7, 2012;
posted January 9, 2012 (Doc. ID 159668); published February 15, 2012

We report on a quantitative elastography technique achieved by combining phase-sensitive optical coherence tomography (PhS-OCT) with the surface acoustic wave (SAW) method. Different from traditional optical coherence elastography, the elastography is achieved by impulse-stimulated SAW, rather than by shear waves. PhS-OCT serves not only as a detector to measure SAW signals but also as a means to provide a cross-sectional image of the sample. The experimental results indicate that the combination of PhS-OCT with SAW is feasible to provide quantitative elastography of heterogeneous tissue samples. © 2012 Optical Society of America

OCIS codes: 350.5030, 170.4500, 170.3880.

The alternation of mechanical properties of biological tissues, especially the stiffness, directly correlates with the tissues' pathological status [1]. Elastography is a noninvasive biomedical imaging technique that can provide elastic as well as anatomic information of the biological tissue. The main idea behind this technology is to combine imaging modalities (e.g., ultrasonic, magnetic resonant, or optical) with different mechanical stimulations (e.g., compression, vibration, or transient stimulation) [2–4]. Mechanical stimulation generates tissue responses in the form of displacement, strain, or vibration, that can be subsequently measured so that the tissue mechanical properties may be evaluated and mapped.

Optical coherence elastography (OCE) [2,5], based on optical coherence tomography (OCT), has increasingly become attractive, as it takes advantage of the high spatial resolution of the OCT imaging modality. The ability of OCE in identifying and localizing small lesions within tissue cannot be achieved by the current ultrasound elastography [1,4] and magnetic resonance elastography [3]. Most of the OCE systems use an external shaker to induce mechanical shear waves that subsequently travel within a sample. Through evaluating the strain rate of shear energy, OCE has been shown capable of differentiating tissues with differing stiffness [2,5,6], delivering a promise to achieve 3 D elastography of superficial human skin [7] for dermatological applications. Notwithstanding, it is still problematic for OCE to provide the Young modulus of the tissue with layered structures. In addition, because OCE totally relies on OCT imaging, it is impossible to provide the elastogram of tissue at a depth beyond the OCT imaging depth, and also it is difficult to image the tissue with relatively low scattering properties.

The surface acoustic wave (SAW) method has been widely used in geology [8] and industrial metrology [9] to evaluate the Young modulus of layered solid materials. A recent study from our group has successfully combined phase-sensitive OCT (PhS-OCT) with the SAW method to evaluate the Young modulus of thick layered biological phantoms and human skin *in vivo* [10,11]. With the SAW method, the measurements at two locations with known separation distance are required so that the SAW phase velocity curves can be obtained, from which the elasticity of the sample is calculated using an inverse procedure. However, it is desirable that the biomechanical properties of the tissue are mapped, i.e., the elastography, to provide direct visualization of the tissue stiffness for ease of biomedical diagnosis, e.g., skin diseases. To fulfill this requirement, this Letter reports on the use of surface wave method, coupled with PhS-OCT, to enable the SAW elastography.

The schematic of the experimental setup was similar to that described in our previous study [10]. Briefly, the system consisted of two main parts: one that generates the SAWs that propagate at the surface of the sample, and another that detects the SAW. The SAW generation was achieved by a homemade metal-rod shaker (~2 mm diameter). It was directly in contact with the sample surface to transmit the vibration and generate the desired surface waves. For this study the shaker generated pulses at ~20 Hz with an ~0.2% duty cycle, producing the SAW with frequencies up to ~10 kHz. A PhS-OCT system was utilized to detect surface wave signals at the tissue surface, in addition to providing real-time imaging of tissue morphology for assisting the determination of the elasticity of the sample. The PhS-OCT is comprised of a superluminescent diode with a central wavelength of 1310 nm and a spectral bandwidth of 46 nm, providing an axial resolution of ~15 μm and a transverse resolution of ~16 μm (in air). The sampling rate was set at ~47 kHz, sufficient to capture the SAW signals (up to 10 kHz).

The PhS-OCT sampled the SAW signals, started at the location 2 mm away from the shaker, and then sequentially moved linearly to locations with 0.5 mm/step, and finally ended at a position 17 mm away from the shaker. In this way, the PhS-OCT sampled 31 locations over the tissue surface that span 15 mm. The frequency-dependent phase velocity curve was then calculated from every two adjacent locations, using an algorithm reported in [10,11]. The relationship between the SAW

frequency-dependent phase velocity, $C_R(f)$ and biomechanical properties can be described as

$$C_R(f) = \frac{0.87 + 1.12\upsilon}{1 + \upsilon}\sqrt{\frac{E(f)}{2\rho(1 + \upsilon)}}, \quad (1)$$

where $E(f)$ denotes the Young modulus at the SAW frequency f, ν is the Poisson ratio, and ρ is the mass density of the material. Compared to the shear wave approach, the surface wave method is more sensitive and directly related to the Young modulus. From Eq. (1), once the phase velocity is obtained, the Young modulus can be deduced, provided that ν and ρ are known *a priori*. We used $\nu = 0.45$ and $\rho = 1060$ kg/m^3, which are valid for the samples, including human skin, in our study [10,11]. The Young modulus curve as a function of frequency is then estimated based on the phase velocity curve calculated from adjacent locations, resulting in an A-line of SAW elastography. After all the adjacent locations are evaluated, a B-scan elastographic image is built, with its horizontal axis representing the spatial extent (i.e., distance, mm) over the sample and the vertical axis representing the SAW frequency (Hz) that is related to the depth. The minimum surface wave velocity that the current system can measure is ~0.011 m/s, determined by the time of SAW traveling between adjacent sampling locations (0.5 mm), corresponding to a Young modulus ~0.45 Pa, which represents the system sensitivity.

In order to coin the above-obtained elastography to the scanned sample, the next step is to convert the SAW frequency into the depth information of the sample. It is known that the surface wave penetration depth (z) is linearly proportional to its wavelength (λ) but inversely related to the frequency of its phase velocity [12]:

$$z \approx \lambda = \frac{C_R}{f}. \quad (2)$$

Thus, the inversion from the frequency contents to the depth information of the sample is a nonlinear process. For a material with layered structures, the surface wave shows a dispersive behavior. The phase velocity in the low-frequency content represents the elasticity of the deeper layer while that in the high-frequency content gives the elasticity of the upper layer of the sample, meaning the phase velocity is not a constant value but varies with the frequency, and the velocity at each frequency corresponds to the elasticity of the sample at a certain depth corresponding to that frequency. The minimum depth that the SAW method can sense is determined by the maximum frequency contained within the detected SAW signal, which is expressed as [13]

$$f_{\max} = \frac{2\sqrt{2}C_R}{\pi r_0}, \quad (3)$$

where r_0 is the radius of the stimulator. From Eqs. (2) and (3), the minimum depth that the surface wave method can detect is only related to the stimulator radius. As the shaker had an ~2 mm radius, the minimum depth of elastography by our system was thus ~1 mm. On the other hand, the maximum depth of SAW elastography can be calculated from Eq. (2) by the lowest frequency content and its corresponding surface wave velocity. Here, the lowest frequency (typically ~1 kHz) was defined by −10 dB from the maximum of the autocorrelation spectrum. Thus, the maximum depth that the current system can sense is ~5 mm because the SAW velocity was typically ~5 m/s at ~1 kHz in our study.

To verify the proposed elastography approach, we first used agar–agar phantoms largely because the agar is not only economical but also can be used to make mechanically heterogeneous samples with relative ease. We first made a double-layered phantom with ~1% agar as the base and ~1.3 mm thick ~2% agar as the top layer into which an ~3% agar was included in its middle region. The gel was mixed with 0.5% Intralipid, giving a scattering background to provide a contrast for OCT imaging. Thus, this phantom possessed mechanical heterogeneity that is sufficient to test the sensitivity of the proposed method to differentiate the localized inclusion of the 3% from the 1% and 2% agar-gel background.

The results are shown in Fig. 1, where (a) is the typical OCT structure image of the phantom that provides important geometrical information and (b) is the resulted SAW elastogram with the quantitative Young modulus given. The OCT image clearly shows the boundaries [marked in Fig. 1(a)] between areas of different agar concentrations, demonstrating the possible mechanical inhomogeneity of the sample, but it is unable to give the elasticity of sample. The mapped elastography by the proposed approach [Fig. 1(b)] distinguished the elasticity of regions with different agar concentrations, with its geometry corresponding well with that observed in Fig. 1(a). The averaged values of the Young modulus at 3%, 2%, and 1% agar concentration regions were, respectively, ~500, ~200, and ~100 kPa, and they agreed well with the values obtained by previous studies where the elasticity of homogeneous phantoms made by different agar concentrations was measured [10,11]. From Fig. 1(b), we can also observe that the interface between the 3% and 1% concentration agar appears at ~4 kHz because there is an apparent transition of the Young modulus in the elastography. Thus, this value of 4 kHz and its associated phase velocity (~5 m/s) can be used to estimate the thickness of the top 3% agar layer, which gives

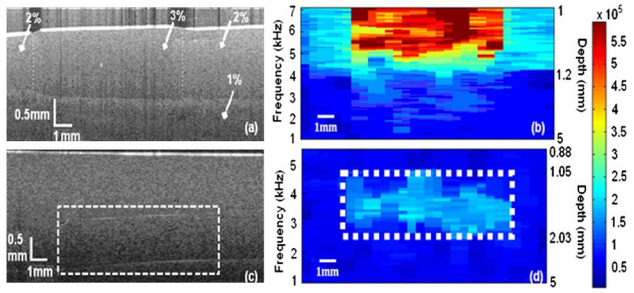

Fig. 1. (Color online) (a) OCT image of the phantom with ~1% agar as the substrate layer, ~2% agar and ~3% agar as upper layer and (b) elastogram of the phantom evaluated from the phase velocity curves. (c) OCT image of the phantom with ~2% agar (outlined by the dashed box) embedded within an ~1% agar background and (d) the resulting elastogram. The color bar represents the value of elasticity (Pa). The same also applies to Fig. 2.

1.2 mm, matched very well with that measured from the OCT image (~1.25 mm).

In order to test if the proposed method is able to detect the elasticity change within sample, another phantom was made with a 2% agar block embedded inside 1% agar-gel. The results are also presented in Fig. 1. The OCT image [Fig. 1(c)] confirmed the 2% agar inclusion with a thickness of ~1 mm, located at ~1.1 mm beneath the surface. Again the SAW elastography [Fig. 1(d)] demonstrated the ability to differentiate the localized mechanical inclusion from the background, with the geometrical appearance of the mechanical heterogeneity matching well with the OCT structure image. From Fig. 1(d), we obtained an averaged Young modulus for 2% agar inclusion of ~200 kPa, while that in the background of ~100 kPa. The upper and lower boundaries of the 2% agar inclusion can be estimated by the frequencies of ~4.5 and ~2.5 kHz, corresponding to ~1.05 and ~2.03 mm from the surface of the phantom and agreed well with the OCT measurement [Fig. 1(c)]. These results demonstrate the feasibility of the proposed method to provide elastography of the mechanically heterogeneous samples.

Finally, we used the proposed SAW elastography method to test on a human forearm skin *in vivo* with a hard nodule in the dermis layer, which can be observed by the OCT image [Fig. 2(a)]. From the OCT image, it can be seen that the hard nodule is ~0.5 mm beneath the surface, but is difficult to provide its size because of the limited imaging depth, which is less than 1 mm. The elastographic image [Fig. 2(b)] distinguished the stiffness between the nodule and background tissue. At the normal human skin, the Young moduli gradually decrease from the surface (200 kPa from ~5 to ~3 kHz, corresponding to depths from ~1.5 to ~2.2 mm, i.e., the dermis layer) into the depth (100 kPa from ~3 to ~1 kHz, corresponding to the depths from ~2.2 to ~4 mm, i.e., subcutaneous fat layer). The Young moduli measured for dermis and subcutaneous fat layers were consistent with those reported in the prior literatures [10,14]. The hard nodule (shown in red) can be easily distinguished in the elastogram as it has a much higher Young modulus than the surrounding tissues, and it reaches to ~1.85 mm deep inside of skin. However, the current system has difficulty providing the mechanical property of the epidermis layer because the minimum depth that we can measure is ~1 mm.

The spatial resolution of SAW elastography is much lower than that of the prior OCE. This is because the latter relies on OCT to perform strain-rate imaging, while the former requires a certain distance for the surface waves to sufficiently disperse so that the phase velocity can be evaluated. Mapping from the phase velocity to the depth information in SAW elastography is unfortunately a nonlinear process, which needs to be further studied in order to provide the elastography in a linear geometrical scale so that it can be directly presented alongside with OCT imaging for ease of use in biomedical applications. Furthermore, the minimum sensing depth of the current system is limited by the size of the stimulator used. This problem may be amendable if a laser source is used to stimulate the surface waves because the laser beam can be easily focused, leading to increased high-frequency contents within the generated SAW signals.

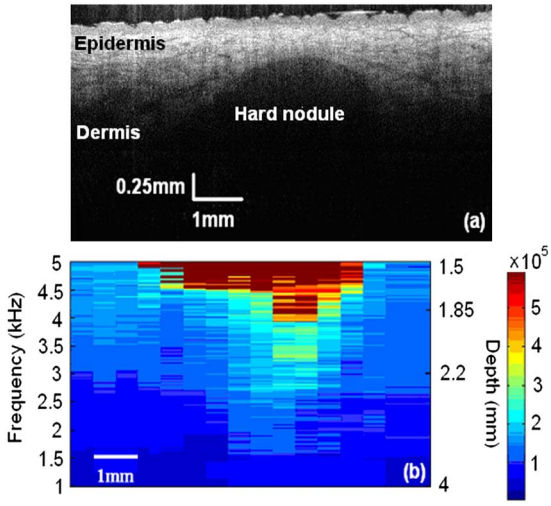

Fig. 2. (Color online) (a) OCT image of human forearm skin *in vivo* with a hard nodule in the middle and (b) the resulting elastogram.

In conclusion, we have demonstrated that the surface wave method can be successfully utilized to quantitatively image and map the elasticity of soft and layered heterogeneous tissues. We used a PhS-OCT system to detect the surface waves generated from a homemade shaker, from which the elastic properties of the tissue are evaluated. Unlike traditional OCE, the proposed SAW elastography is independent of OCT imaging, but it utilizes OCT to provide complementary morphological information of the tissue that can be particularly useful for diagnostic purposes.

References

1. J. Ophir, I. Cespedes, H. Ponnekanti, Y. Yazdi, and X. Li, Ultrason. Imag. **13**, 111 (1991).
2. C. Sun, B. Standish, and V. X. D. Yang, J. Biomed. Opt. **16**, 043001 (2011).
3. T. Elgeti, M. Laule, N. Kaufels, J. Schnorr, B. Hamm, A. Samani, J. Braun, and I. Sack, J. Cardiovasc. Magn. Reson. **11**, 44 (2009).
4. T. Rago, F. Santini, M. Scutari, A. Pinchera, and P. Vitti, J. Clin. Endocrinol. Metab. **92**, 2917 (2007).
5. J. M. Schmitt, Opt. Express **3**, 199 (1998).
6. R. K. Wang, Z. Ma, and S. J. Kirkpatrick, Appl. Phys. Lett. **89**, 144103 (2006).
7. B. F. Kennedy, X. Liang, S. G. Adie, D. K. Gerstmann, B. C. Quirk, S. A. Boppart, and D. D. Sampson, Opt. Express **19**, 6623 (2011).
8. S. Nazarian and M. R. Desai, J. Geotech. Eng. **119**, 1094 (1993).
9. A. Neubrand and P. Hess, J. Appl. Phys. **71**, 227 (1992).
10. C. Li, G. Guan, R. Reif, Z. Huang, and R. K. Wang, J. R. Soc. Interface, doi:10.1098/rsif.2011.0583 (to be published).
11. C. H. Li, Z. H. Huang, and R. K. K. Wang, Opt. Express **19**, 10153 (2011).
12. H. C. Wang, S. Fleming, Y. C. Lee, S. Law, M. Swain, and J. Xue, Opt. Express **17**, 15592 (2009).
13. Y. H. Sohn and S. Krishnaswamy, Ultrasonics **39**, 543 (2002).
14. P. G. Agache, C. Monneur, J. L. Leveque, and J. De Rigal, Arch. Dermatol. Res. **269**, 221 (1980).